Differentiation and dose-ranging assessment of midbrain dopaminergic neurons from human pluripotent stem cells for treatment of Parkinson's disease

Chan Wook Park

The Graduate School
Yonsei University
Department of Medicine

Differentiation and dose-ranging assessment of midbrain dopaminergic neurons from human pluripotent stem cells for treatment of Parkinson's disease

A Dissertation Submitted
to the Department of Medicine
and the Graduate School of Yonsei University
in partial fulfillment of the
requirements for the degree of
Doctor of Philosophy in Medical Science

Chan Wook Park

June 2024

연세대학교
YONSEI UNIVERSITY

**This certifies that the Dissertation
of Chan-Wook Park is approved.**

Thesis Supervisor   Dong-Wook Kim

Thesis Committee Member   Phil-Hyu Lee

Thesis Committee Member   Dae-Sung Kim

Thesis Committee Member   Dong-Youn Hwang

Thesis Committee Member   Seok-Jong Chung

**The Graduate School
Yonsei University
June 2024**

ACKNOWLEDGEMENTS

TABLE OF CONTENTS

LIST OF FIGURES

LIST OF TABLES

ABSTRACT

Differentiation and dose-ranging assessment of midbrain dopaminergic neurons from human pluripotent stem cells for treatment of Parkinson's disease

Human pluripotent stem cell (hPSC)-derived midbrain dopaminergic (mDA) progenitor transplantation is a promising therapeutic strategy for Parkinson's disease (PD). For clinical applications, it is crucial to develop a differentiation method that produces mDA progenitors with high safety and efficacy from hPSCs. In this study, a differentiation protocol was developed using four small molecules, including dual-SMAD inhibiton and subsequent treatment with smoothened agonist (SAG) and CHIR99021 to produce high purity mDA progenitors from human embryonic stem cells. Preclinical assessments showed that mDA progenitors transplanted into hemi-parkinsonian rats differentiated into functional DA neurons. The transplanted mDA neurons normalized motor asymmetry, increased [^{18}F]F-DOPA uptake, and elevated dopamine levels at 16 weeks post-transplantation. Immunohistochemical analysis demonstrated low proliferation rates and no abnormal overgrowth of the transplanted mDA progenitors, ensuring safety. Additionally, before conducting clinical trials, it is necessary to determine the range of minimal cell doses with therapeutic effect. Various doses of mDA progenitors were transplanted into hemi-parkinsonian rats, and a significant dose-dependent behavioral improvement was observed with a minimal effective dose range of 5,000–10,000 mDA progenitor cells. These results provided insights into determining a low cell dosage (3.15 million cells) for human clinical trials.

I. INTRODUCTION

Parkinson's disease (PD) is the second most prevalent neurodegenerative disease, impacting approximately 1% of the population over 60. Characterized by motor symptoms known as Parkinsonism, which include bradykinesia, rigidity, and resting tremor, the primary cause is the degeneration of midbrain dopamine (mDA) neurons in the substantia nigra pars compacta (SNpc).[1] Consequently, dopamine replacement medications have become the standard treatment approach. While these medications initially improve motor symptoms in PD patients, their efficacy diminishes as the disease progression. Long-term use often leads to side effects such as dyskinesia and motor fluctuations. In cases where these side effects significantly impair function despite optimal medication dosing, advanced therapies like deep brain stimulation (DBS) might be considered.[2] However, the effectiveness of such surgical treatments also declines over time, and DBS procedures are associated with various complications, including hardware-related infections, postoperative cognitive impairment, and battery failure.

In an effort to circumvent the limitations of conventional therapies, cell therapy has emerged as a promising alternative, aiming to directly replace the progressively lost mDA neurons. Since 1988, numerous clinical trials have explored fetal cell transplantation, facing challenges such as immunologic reactions to allogenic transplantation, ethical issues surrounding the use of aborted fetuses, and the use of the non-homogeneous cells lacking dopaminergic neurons.[3, 4] Despite these hurdles, some patients undergoing fetal nigral cell

transplantation have exhibited clinical improvement without serious adverse effects.[5] Randomized, double-blind studies conducted in 2001 and subsequent trials in 2005 have demonstrated functional improvements and enhanced recovery in PD patients.[6, 7] However, the inconsistency of results underscores the necessity for a refined cell-based approach that guarantees the production of a sufficient number of well-defined mDA cells alongside a standardized cell preparation and transplantation protocol.[8]

Pioneering work by Roy et al. in 2006, and subsequent advancements by Cho et al. in 2008, have significantly advanced the field, demonstrating the feasibility of differentiating human embryonic stem cells (hESCs) into dopaminergic neurons and their potential for substantial and long-lasting restoration of motor function in parkinsonian rat models.[9, 10] These technological breakthroughs have facilitated the efficient generation of mDA neurons from human pluripotent stem cells (hPSCs), such as hESCs and induced pluripotent stem cells (iPSCs), heralding a new era of hPSC-based transplantation therapies for PD.[11-17] Numerous studies have shown that hPSC-derived mDA progenitors integrate well into the host brain and mature into functional mDA neurons when grafted into parkinsonian animal models, significantly improving motor functions.[18, 19] Additionally, a recent study reported stable or improved clinical symptoms in a PD patient following autologous transplantation of hiPSC-derived mDA progenitors 24 months post-transplantation, with early clinical trials of hiPSC-derived and hESC-derived mDA progenitors underway in various regions.[20-23]

The first step in bringing cell transplantation for PD to clinical use is establishing

an optimal protocol for differentiating hPSCs into mDA progenitors with high efficacy and safety. Additionally, a critical step in translating cell transplantation for PD into clinical practice is determining an optimal range of cell doses for transplantation, to serve as a reference for human trials. This thesis presents an optimized method to produce high purity mDA progenitors and identifies a dose range that produced a therapeutic effect in toxin-induced hemi-parkinsonian rats, offering vital insights into the appropriate cell dosage for future human trials.

II. MATERIALS AND METHODS

1. Animals

The efficacy tests were performed at Yonsei Biomedical Research Institute, Yonsei University College of Medicine. All animal experiments were approved by the Institutional Animal Care and Use Committees of Yonsei University Health System. Adult Sprague– Dawley (SD) rats (Crl:CD, Orient Bio, 200–250 g, 7–8 weeks old) were used.

The researchers who performed the experiments were all blinded to group assignment. In all studies, animals were randomized to the different groups.

2. Cell lines

Clinical grade hESCs, SNU-hES32, were supplied by the medical research center (Institute of Reproductive Medicine and Population), Seoul National University, South Korea. Sparse embryos with an embryo disposition agreement were frozen in July 27, 1998, by the Mizmedi Hospital, Seoul, South Korea. The embryos were supplied by the medical research center (Institute of Reproductive Medicine and Population), Seoul National University, on October 29, 2009, and were thawed and cultured on a foreskin feeder layer by whole-embryo culture to establish an hESC line on June 4, 2010. The inner cell mass was mechanically dissected and cultured in Dulbecco's modified Eagle's medium/nutrient mixture F12 (DMEM/F12) medium. The hESC line was established at passage 2 and

registered as SNU-hES32 by the Korea Centers for Disease Control and Prevention on December 20, 2010 (Registration number: hES12010051). The hESC line exhibited a normal karyotype (46, XY) and identical nucleus and mitochondria DNA fingerprinting to the egg and sperm donors. Expression of pluripotency genes and surface markers, three-germ-layer differentiation, virus or bacteria contamination, ABO typing (type B) and HLA typing were further assessed.

3. Human embryonic stem cell culture and differentiation

Undifferentiated hESCs, SNU-hES32, were seeded on WebTrix™ 60-mm dishes (Amolifescience, Seoul, South Korea) and TeSR™2 medium (Stemcell Technologies, Vancouver, Canada) was replenished daily. On differentiation day (DD) 0, cells were treated with 5 µM dorsomorphin (DM; Millipore Sigma, St. Louis, MO, USA) and 5 µM SB431542 (SB; Millipore Sigma) to prime them for neuroectodermal specification. On DD1, cells were divided into 1.5 mm × 1.5 mm-size sections, using a 1-ml syringe, and detached with collagenase (Animal-Free Types AFC; Worthington Industries, Columbus, OH, USA). The cell fragments formed 3D cell aggregates and were cultured in suspension on 60-mm Petri dishes in StemFit Basic03 medium (SF03; Ajinomoto, Tokyo, Japan) with DM and SB for neuroectodermal specification. On DD4, in the late phase of neuroectodermal specification, ventral mesencephalic regional specification was simultaneously induced by introducing 1 µM smoothened agonist (SAG; Millipore Sigma), and 2 µM CHIR99021 (CHIR; Miltenyi Biotec, Bergisch Gladbach, North Rhine-

Westphalia, Germany), along with SF03 containing DM and SB, for a duration of 2 days. On DD6, 3D cell aggregates were placed on 60-mm dishes coated with biolaminin 521 (Biolamina, Sunbyberg, Sweden) in DMEM/F12 (Thermo Fisher Scientific) with N-2 supplement (N-2; Thermo Fisher Scientific), 20 ng/ml CTS recombinant fibroblast growth factor basic (Thermo Fisher Scientific), 20 μg/ml insulin solution human (Millipore Sigma), 1 μM SAG, and 2 μM CHIR for neural rosette formation. On DD10, neural rosettes were incubated with accutase (Millipore Sigma) and split using a cell scraper. Cells were plated in T25 flasks in DMEM/F12 with N-2, B-27 supplement (B27; Thermo Fisher Scientific), 1 μM SAG, and 2 μM CHIR. On DD13, cells were detached with accutase and plated in T25 flasks in DMEM/F12 with N2 and B27. Additionally, SAG and CHIR were continuously supplemented for a further 6 days, to reinforce maintenance of ventral mDA identity. On DD19, cells were seeded in T25 flasks in DMEM/F12 with N2 and B27. On DD25, cells were detached with accutase for transplantation or maturation into mDA neurons. To differentiate the dopaminergic progenitors on DD25, cells were cultured in NBG media (DMEM/F12 with N2, B27, and G21 supplements; GeminiBio) with 1 μM DAPT (Millipore Sigma) for 3 days. Cells were further differentiated in NBG media with 10 ng/ml brain derived neurotrophic factor (BDNF; ProSpec, Rehovot, HaMerkaz, Israel), 10 ng/ml glial cell-derived neurotrophic factor (GDNF; ProSpec), 200 μM ascorbic acid (Millipore Sigma), and 1 μM dibutyryl-cAMP (Millipore Sigma).

4. Real-time qPCR analyses

Total RNA was isolated using an RNA extraction kit (Qiagen, Hilden, Germany). Complementary DNA was synthesized from 1 μg of total RNA, quantified by nanodrop spectrophotometer, and prepared using PrimeScript RT Master Mix (Takara Bio, Kusatsu, Shiga, Japan). Real-time qPCR was performed with a thermal cycler using a PCR Master Mix and primers as listed in **Table 1**.

5. Immunocytochemistry

Cells fixed with 4% PFA were permeabilized with 0.1% Triton X-100, blocked with 2% BSA, and incubated overnight at 4 ℃ with primary antibodies (**Table 2**). The primary antibody-stained cells were incubated with fluorescence-tagged secondary antibodies for 1 h at room temperature. Images were obtained using an IX73 inverted microscope (Olympus, Shinjuku City, Tokyo, Japan) or a laser scanning microscope (LSM) 710 (Carl Zeiss AG, Oberkochen, Baden-Wurttemberg, Germany).

Table 1. Real-time qPCR primer sequences

Primer	Sequence
EN1 forward	CTG GGT GTA CTG CAC ACG TT
EN1 reverse	GCT TGT CCT CCT TCT CGT TC
FOXA2 forward	CCG TTC TCC ATC AAC AAC CT
FOXA2 reverse	GGG GTA GTG CAT CAC CTG TT
LMX1A forward	CAG CAG CAA GAT CAG CAG AA
LMX1A reverse	AGG GGT TCA TGA TTC CTT CC
PITX3 forward	AGG AGA TCG CCG TGT GGA CCA
PITX3 reverse	CCG CGA AGC TGC CTT GC ATA G

Table 2. Antibodies

Antibodies	SOURCE	IDENTIFIER
AFP	Santa Cruz	Cat#sc-8399
BARHL1	NOVUS	Cat#NBP1-86513
BRACHYURY	R&D systems	Cat#AF2085
CALBINDIN	Millipore	Cat#AB1778
FOXA2	Abcam	Cat#AB108422
FOXA2	Santa Cruz	Cat#sc-374376
GAD65	Millipore Sigma	Cat#AB5082
GFAP	Millipore	Cat#IF03L
GFAP	Millipore	Cat#MAB360
GIRK2	Almone Labs	Cat#APC-006
HNA	Millipore	Cat#MAB1281
Ki-67	Abcam	Cat#Ab15580
LMX1A/B	Millipore	Cat#AB10533
MAP2	Millipore	Cat#AB5622
NCAM	Santa Cruz	Cat#sc-106
NURR1	Santa Cruz	Cat#sc-990
OTX2	R&D systems	Cat#AF1979
PITX3	NOVUS	Cat#NBP1-92274
TH	Sigma	Cat#T1299
TH	Pel-freez	Cat#P40101
TH	Pel-freez	Cat#P60101
5-HT	ImmunoStar	Cat#20080
LMX1A	Santa Cruz	Cat#sc-54273
SOX17	R&D Systems	Cat#AF1924
SMAa	Millipore Sigma	Cat#A5228
COL1A1	R&D systems	Cat#AF6220
TTR	Abcam	Cat#AB92469
AADC	Chemicon	Cat#AB1569

6. Dopamine-release test

Matured cells (DD56) were incubated in low KCl solution (2.5 mM $CaCl_2$, 11 mM glucose, 20 mM HEPES-NaOH, 4.7 mM KCl, 1.2 mM KH2PO4, 1.2 mM MgSO4, and 140 mM NaCl) at 37 ℃ for 2 min. The solution was subsequently replaced with a high-KCl solution (2.5 mM $CaCl_2$, 11 mM glucose, 20 mM HEPES-NaOH, 60 mM KCl, 1.2 mM KH_2PO_4, 1.2 mM $MgSO_4$, and 85 mM NaCl), and the cells were further incubated at 37 ℃ for 15 min. The solution was collected in 15-ml tubes and centrifuged for 1 min at 2000 rpm to remove the debris. The supernatant was collected in 1.5-ml tubes and stored at 80 ℃ until use. Dopamine (DA) concentration was measured using a DA ELISA kit (Abnova, Taipei City, Taipei, Taiwan) according to the manufacturer's instructions.

7. Cell transplantation into parkinsonian rat model

Adult SD rats were used for transplantation (200–250 g; Orient Bio, Gyeonggi-do, South Korea). Zoletil (30 mg/kg; Virbac, Carros, France) and Rompun (10 mg/kg; Bayer, Leverkusen, Germany) were used for anesthesia. Rat medial forebrain bundles were stereotactically injected with 3 ml of 30 mM 6-hydroxydopamine hydrochloride (OHDA) (coordinates: AP −4.0, ML −1.3, and DV −7.0). After 4 weeks, cell suspension (4 ml; a total of 350,000, 100,000, 25,000, 10,000, or 5,000 cells) or the vehicle (4 ml; phosphate buffered saline, PBS) was stereotactically injected into the striatum of parkinsonian rats (coordinates: AP +0.8, ML −3.0, and DV −4.0/−5.0). The injection rate was 1 ml/min

for each coordinate, and the Hamilton syringe remained in place at each injection site for 2 min after injection. Cell suspensions were stored at 4 ℃ and transplanted within 3 h after cell dissociation. Starting from 2 days before transplantation until the scarification, cyclosporine A (10 mg/kg) was injected into the intraperitoneal cavity daily.

8. Rat behavior analysis

The amphetamine-induced rotation test was performed 30 min after the intraperitoneal injection of dextroamphetamine (D-amphetamine; Millipore Sigma). Rotations per minute ipsilateral or contralateral to the 6-OHDA lesioned striatum were counted. The tests were performed before transplantation and every 4 weeks until 16 or 24 weeks post-transplantation.

9. Animal termination and immunohistochemistry

Each rat received 350,000 cells (n = 4) or vehicle (n = 5) to investigate the therapeutic efficacy. They were sacrificed 16 weeks after transplantation. Rats transplanted with a total of 100,000 (n = 5), 25,000 (n = 4), 10,000 (n = 7), or 5,000 cells (n = 7) or the vehicle (n = 9) for the dose-response test were sacrificed 24 weeks post-transplantation. Rats were anesthetized prior to sacrifice and were fixed by transcardial perfusion with 0.9% saline solution followed by 4% PFA. The brains were post-fixed with 4% PFA and then with 15% sucrose, followed by 30% sucrose. Fixed brains were embedded in Tissue-Tek®

O.C.T. compound (Sakura Finetek, Torrance, CA, USA) and coronally cryosectioned at 40-mm (fixed brains 16 weeks after transplantation) or 20-mm (fixed brains 24 weeks after transplantation). For stereology analysis, 3,3′-diaminobenzidine (DAB) staining for tyrosine hydroxylase (TH; 1:1000) and human neural cell adhesion molecule (hNCAM; 1:100) was performed using the avidin–biotin complex-horseradish peroxidase (ABC-HRP; Maravai LifeSciences, San Diego, CA, USA) and DAB substrate kits (GBI Labs, Bothell, WA, USA) according to the manufacturer's instructions. Hematoxylin staining was performed subsequently. The slides stained with DAB and hematoxylin were scanned using Aperio® AT2 (Leica Biosystems, Wetzlar, Germany).

For immunofluorescence staining, the brain sections were blocked with 3% BSA-PBS solution with 0.3% Triton X-100 for 1 h at room temperature, incubated with the primary antibodies (**Table 2**) overnight at 4 ℃, followed by incubation with the fluorescent conjugated secondary antibodies for 2 h at room temperature, and then stained with 4′,6-diamidino-2-phenylindole (DAPI). The slides were tilescanned at 400× magnification using an LSM 980 confocal microscope (Carl Zeiss, Oberkochen, Germany). Fluorescent-stained cells were counted manually using Image J software (v1.53c; National Institutes of Health, Bethesda, MD, USA), and the total numbers were calculated by multiplying with 24 for series number (1:24) and corrected by applying factors to minimize overcounts due to the presence of split particles in multiple sections.[24, 25]

10. Dopaminergic fiber volume estimation

For dopaminergic fiber volume quantification, injected striatal regions of scanned TH-DAB staining were analyzed. The nucleus accumbens (NAc) and the dorsal striatum (DS) were delineated according to anatomical landmarks in the rat brain atlas.[26] The area of each section was analyzed using the Aperio® ImageScope (v12.3; Leica Biosystems), as described elsewhere.[17, 27] The Positive Pixel Count v9 algorithm with standard parameters for brown color quantification was used, and strong positive intensities of the grafts were included in the measurements. The area of each section was extrapolated in every section of the 1:24 series, and the volumes were calculated using Cavalieri's principle, given the known distance between each section and the known section thickness.[28]

11. [^{18}F]F-DOPA PET/CT image acquisition and analysis

The 3,4-dihydroxy-6-[^{18}F]fluoro-L-phenylalanine ([^{18}F]F-DOPA) positron-emission tomography (PET)/computed tomography (CT) images were acquired at 2 weeks before and at 4, 8, 12, 16 weeks after cell transplantation into parkinsonian rats. Cell suspension (4 ml; 350,000 cells) or the vehicle (4 ml; PBS) was stereotactically injected into the striatum of parkinsonian rats. In each set, four parkinsonian rats were used. Half of the rats were injected with cell suspension and the rest of them were injected with vehicle. Four sets of parkinsonian rats were used for [^{18}F]F-DOPA PET/CT imaging.

Imaging was conducted under general anaesthesia using isoflurane in 0.6 L/min O_2 and 0.4 L/min N_2O_2. Then, 10 mg/kg carbidopa (Millipore Sigma), followed by 10 mg/kg entacapone (Millipore Sigma) were injected intravenously; 30 min after injection of

carbidopa and entacapone, 18.5 ± 7.1 MBq (mean $\pm$ SD) of [^{18}F]F-DOPA was injected as a bolus via the tail vein. Dynamic PET imaging lasted 2h. To acquire [^{18}F]F-DOPA PET/CT images, a nanoScan PET/CT scanner (Mediso Medical Imaging Systems, Budapest, Hungary) was used, with PET/CT data acquired using Nucline v2.01 acquisition software (Mediso Medical Imaging Systems). Prior to radiotracer injection, a scout-view CT image was acquired. Dynamic PET imaging commenced upon injection of [^{18}F]F-DOPA. After PET imaging, CT data were acquired (Trajectory semi-circular, maximum field-of-view, 480 projections, 55 kVp and 300 ms, binning 1:4) and used for attenuation correction of PET data.

The PET data was reconstructed and extended from the olfactory bulbs to the caudal border of the heart. 3D dynamic reconstruction was conducted using the Tera-Tomo 3D reconstruction method (Mediso Medical Imaging Systems). The settings included a coincidence mode of 1–3, a voxel size of 0.4 mm × 0.4 mm × 0.4 mm, 4 iterations and 6 subsets. Correction for scatter, attenuation, and randoms was applied. Data were reconstructed into frames comprising six frames of 30 s, three frames of 60 s, two frames of 120 s, and 22 frames of 300 s. the [^{18}F]F-DOPA uptake in each side of the bilateral striatum and cerebellum was measured with PMOD software version 4.1 (PMOD Technologies, Zurich, Switzerland). The standardized uptake value ratio (SUVr) of the striatum was measured using the SUV of the cerebellum as a reference. The SUVr before cell injection was compared with the SUVr after the cell injection.

12. Measuring dopamine concentration in rat brains using HPLC with PDA detection

The dopamine concentration in rat brains was measured according to the previously described methodology.[29] Briefly, the brains of rats were removed from the skull, washed in ice-cold sodium chloride (0.9%), and sectioned to isolate the bilateral striatum. The samples were weighed, homogenized in ice-cold 0.2 M $HClO_4$ solution (10 mL/mg tissue, Thermo Fisher Scientific), and centrifuged for 20 min (12,000 ×g at 4 ℃). The supernatants were filtered and stored at -80 ℃ for 7 days. Chromatographic separation was performed using a Hypersil Gold C-18 column (250 × 2.1 mm, 5 mm, Thermo Fisher Scientific). The mobile phase consisted of 5 mM $HClO_4$ solution containing 5% acetonitrile (Thermo Fisher Scientific). The high-performance liquid chromatography (HPLC) equipment with a Modl Nanospace SI-2/3001 pump and a 3004 column oven with a 10-mL fixed loop (Shiseido, Tokyo, Japan), the photodiode array (PDA) detector, a Model Dionex PDA-100 (Sunnyvale, CA, USA), and the dsChromn program (Donam Instruments, Seoul, South Korea) were used.

13. Quantification and statistical analysis

For the dose-response tests, statistical analyses were performed using Statistical Package for Social Sciences (v26.0; IBM, Armonk, NY, USA). Amphetamine-induced rotation test results were analyzed by one-way Analysis of Variance (ANOVA) with the

Bonferroni post-hoc test. Linear and logarithmic regressions were performed for data from

immunohistochemical analyses. Values of $p < 0.05$ were considered statistically significant.

III. RESULTS

1. Differentiation of mDA progenitors from hPSCs

For this study, a clinical-grade hESC line (SNU-hES32) established and characterized in the medical research center (Institute of Reproductive Medicine and Population) of Seoul National University was used. To produce mDA progenitors, a differentiation protocol consisting of four stages was developed **(Figure 1)**. Briefly, hESCs were exposed to 5 µM DM and 5 µM SB for 1 day immediately prior to initiating differentiation (stage 1). Subsequently, neural differentiation was induced by culturing them as cell aggregates in suspension under dual-SMAD inhibition for the next 5 days (stage 2; 3D-culture). Following 3D culture, the cell aggregates were plated on laminin-coated dishes and cultured for 4 days (stage 3). At this point, the emerging rosette-like columnar cell clumps were manually isolated and replated on the plate after trituration (stage 4). Concurrently, regional specification toward a ventral mesencephalic fate was initiated, starting from DD 4 to DD19, by treating the cells with 1 µM SAG and 2 µM CHIR for 15 days for ventral mDA neurons. The cells were subjected to an additional 6-day differentiation to reach a stage equivalent to DD25 (**Figure 1)**.

The optimized protocol successfully produced cells expressing FOXA2 (99.61% ± 0.12%) and LMX1A/B (99.87% ± 0.04%) **(Figure 2A)**. A majority of cells expressed mDA markers (FOXA2, LMX1A/B and OTX2), and BARHL1+ cells (potential subthalamic nucleus cell progenitors) remained undetected **(Figure 2B)**. Real-time qPCR

analysis also demonstrated that mDA markers were consistently expressed at high levels in

mDA progenitor populations during this period (**Figure 3**).
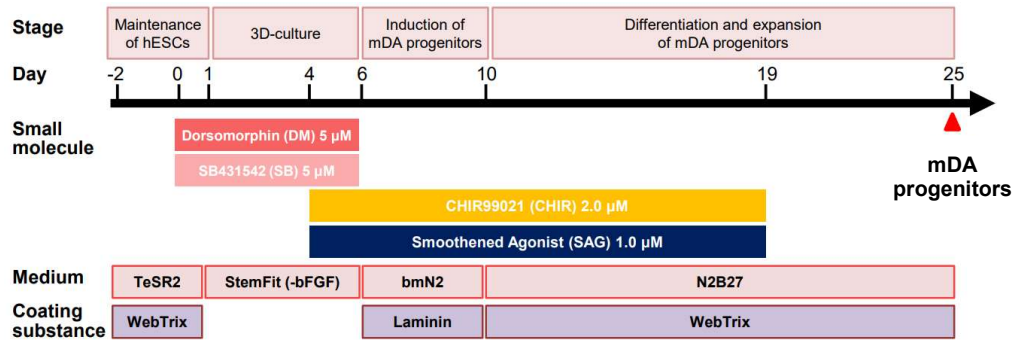
Figure 1. Overview of mDA progenitor differentiation protocol. hESCs were treated with 5 µM DM and 5 µM SB for 1 day. Neural differentiation was then induced using dual-SMAD inhibition for the following 5 days. Starting from DD 4 to DD19, regional specification towards a ventral mesencephalic fate was achieved by treating the cells with 1 µM SAG and 2 µM CHIR for 15 days, aiming to generate ventral mDA progenitors.

A

B
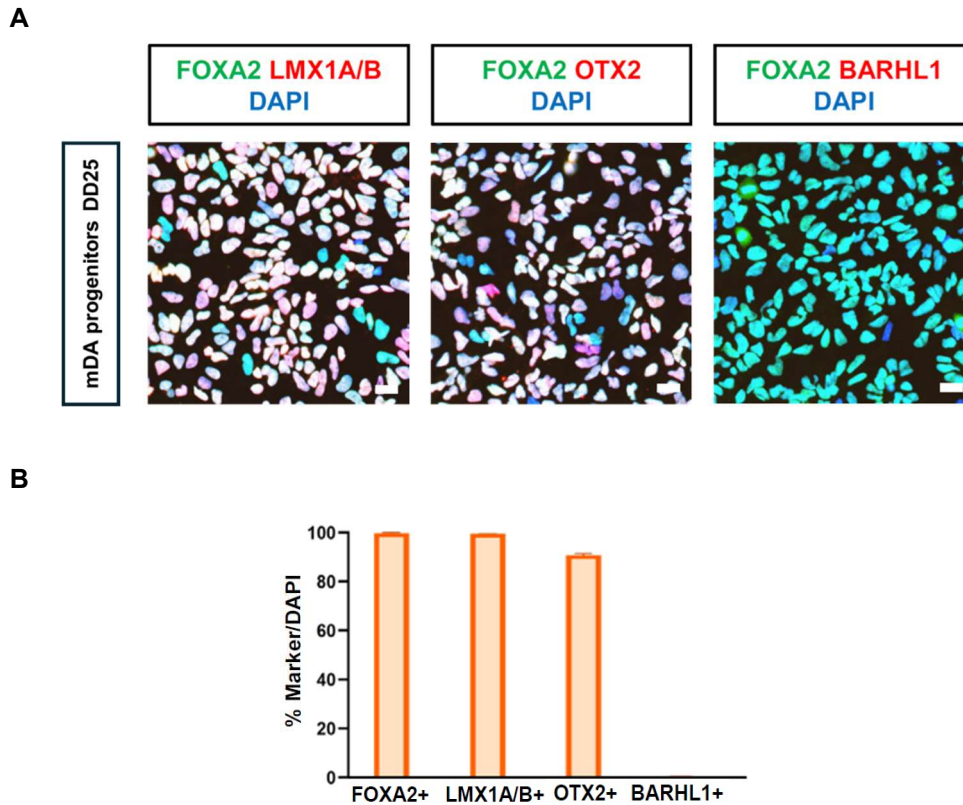
Figure 2. Characterization of mDA progenitors derived from hPSCs with immunocytochemistry. (A) Representative immunofluorescence images of mDA progenitors on DD25, analyzing the expression of ventral diencephalic/mesencephalic markers (FOXA2, LMX1A/B, OTX2, and BARHL1). Scale bars, 20 μm. (B) Quantification of the cells expressing the ventral diencephalic/mesencephalic markers in the mDA progenitors on DD25. Data represent the mean + SE of three independent experiments.
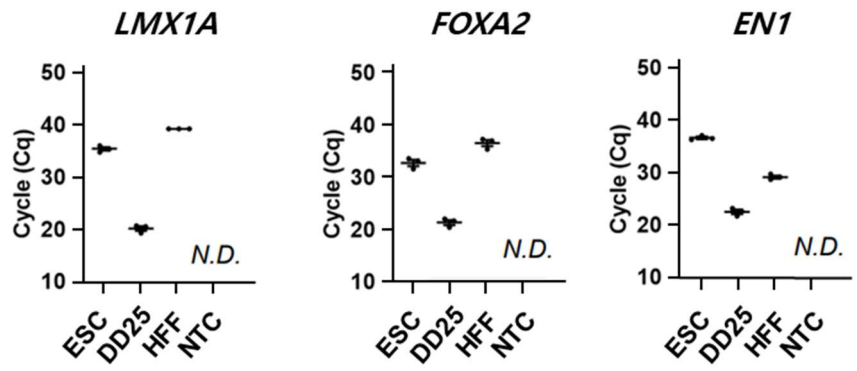
Figure 3. Characterization of mDA progenitors derived from hPSCs with real-time qPCR. The result of real-time qPCR for mDA markers (*LMX1A*, *FOXA2*, and *EN1*) in the mDA progenitors on DD25.

2. Differentiation of mDA neurons from mDA progenitors

Next, the maturation of the cells was tested after differentiating them for an additional 4 weeks. Immunocytochemistry on DD53 revealed frequent TH+ cells co-expressing microtubule-associated protein 2 (MAP2) and ventral mDA markers, including LMX1A and FOXA2 (**Figure 4A and 4B**). TH+ cells also co-expressed several markers important for the mDA neuronal phenotype and function, such as NURR1, PITX3, AADC, CALB, and GIRK2 (**Figure 4A and 4B**). Robust gene expression of mDA markers (*LMX1A*, *FOXA2*, *EN1*, and *PITX3*) in the mDA neuronal population was verified using real-time qPCR analysis (**Figure 5**). At DD60, mDA neurons exposed to a highly concentrated potassium solution secreted more dopamine than those exposed to a low potassium concentration or submerged in culture media (**Figure 6)**, indicating depolarization-induced dopamine release. These data collectively indicate that mDA progenitors produced as described above have the potential to differentiate into functional mDA neurons.

A
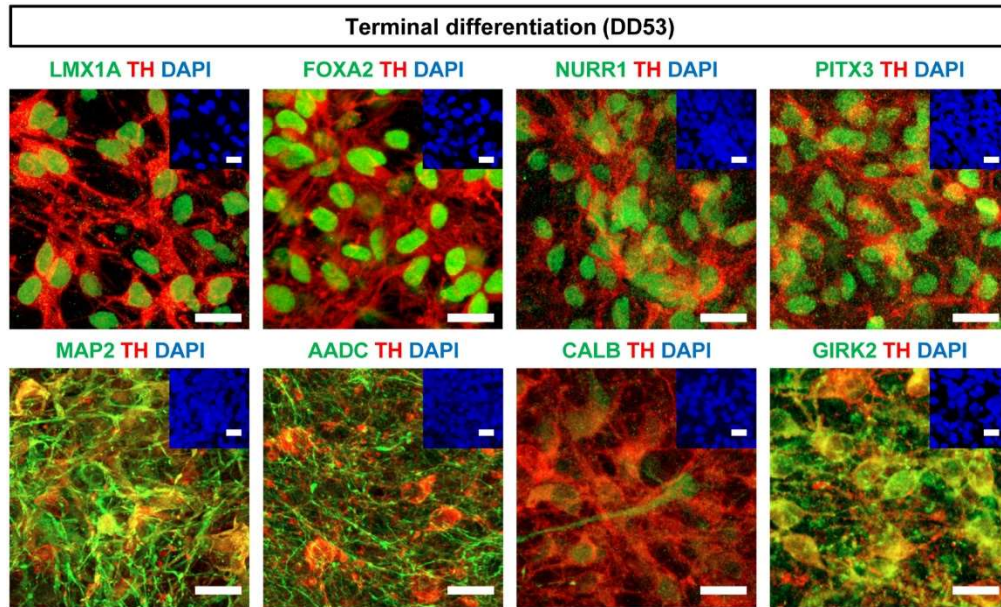
B
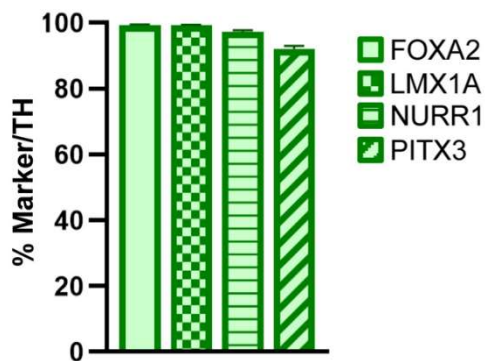
Figure 4. Characterization of mDA neurons derived from mDA progenitors with immunocytochemistry. (A) Immunocytochemical analysis of mDA neurons on DD53. Scale bars, 20 μm. (B) Quantification of FOXA2+, LMX1A+, NURR1+, and PITX3+ cells among TH+ cells, respectively. Data represent the mean + standard deviation (SD) of four independent experiments.
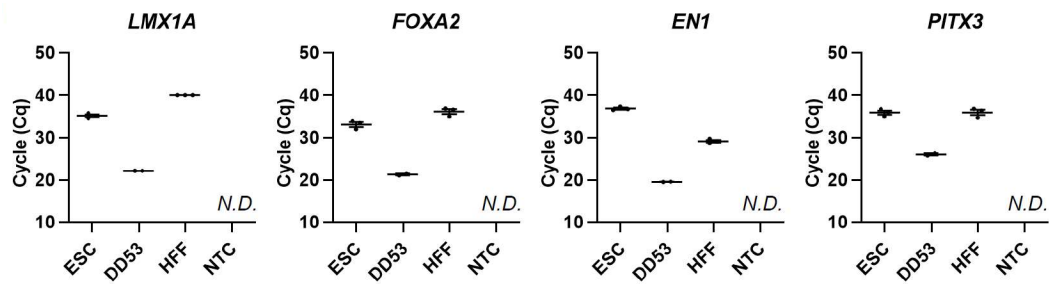
Figure 5. Characterization of mDA neurons derived from mDA progenitors with real-time qPCR. The results of real-time qPCR for mDA markers (*LMX1A*, *FOXA2*, *EN1*, and *PITX3*) in the mDA neurons on DD53. Cq of each marker were normalized to *GAPDH* expression. Data represent the mean ± SE of normalized Cq. *N.D.*, not detected; ESC, undifferentiated hESCs; HFF, human foreskin fibroblasts; NTC, no template control.
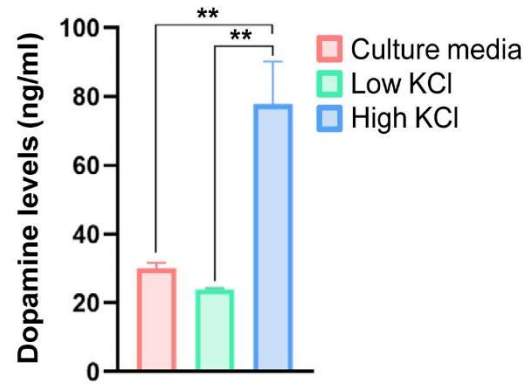
Figure 6. Characterization of mDA neurons derived from mDA progenitors with dopamine-release test. Quantification of dopamine levels in the culture media conditioned in DD60 cultures and under potassium-induced dopamine release. [**]$p < 0.01$, one-way ANOVA with Sidak's multiple comparison test. Data represent the mean + SD of four independent experiments.

3. Transplantation of DA progenitors can reverse a motor deficit in parkinsonian rats

To investigate the therapeutic efficacy of the mDA progenitors, cells were unilaterally transplanted into the striatum of 6-OHDA lesioned parkinsonian rats (350,000 cells per rat). An amphetamine-induced rotation test was performed every 4 weeks. Animals grafted with the mDA progenitors showed a significant reduction in rotational asymmetry at 16 weeks post-grafting (**Figure 7A**). Histological examination revealed that the transplanted cells formed a TH-enriched graft, extending toward the host striatum (**Figure 7B**). These TH+ cells were also HNA+ (**Figures 8A and 8B)**, indicating that they were derived from the grafted cells. Punctate synaptophysin signals were noted, situated on presynaptic terminals, both on the soma and dendrites of the engrafted TH+ (HNA+TH+) neurons. This observation serves as supporting evidence for host-to-graft innervation (**Figures 9)**.

A
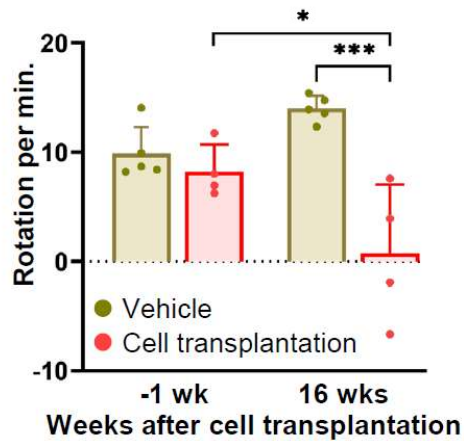
B
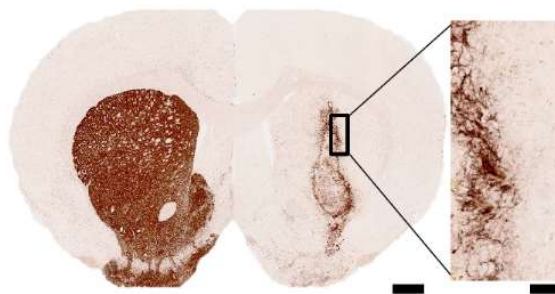
Figure 7. Efficacy of mDA progenitors in the rodent PD model with behavior test. (A) An amphetamine-induced rotation test was performed 1 week before and 16 weeks after mDA progenitors administration. Data represent the mean + SD. $^*p < 0.05$, $^{***}p < 0.001$, two-way ANOVA with Sidak's multiple comparison test. (B) Representative images of DAB-staining for TH in the grafts within the host striatum at 16 weeks after cell administration. Scale bar in the low-magnification image, 1 mm; scale bar in the high-magnification image, 20 μm.

A
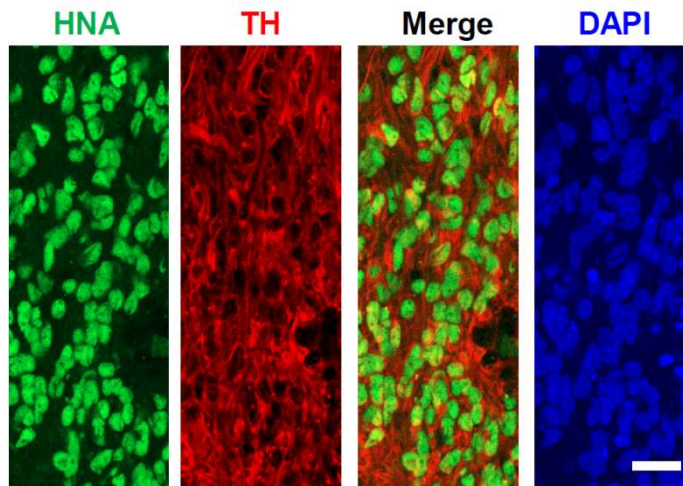
B
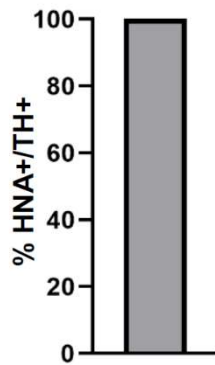
Figure 8. Efficacy of mDA progenitors in the rodent PD model with immunohistochemistry. (A) Immunohistochemical analysis of expression of HNA (green) and TH (red) in the grafts. Scale bar, 20 μm. (B) Quantification of HNA+ cells among the TH+ cells in the grafts. Data represent the mean + SD.
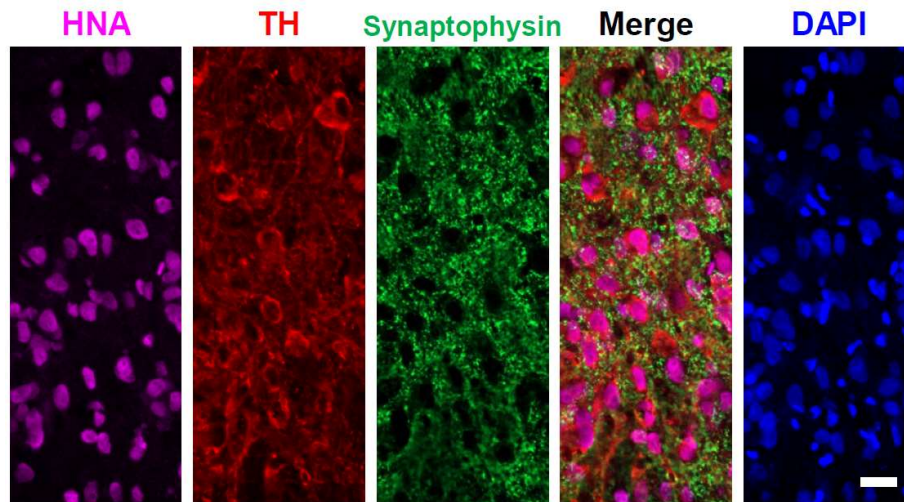
Figure 9. Host-to-graft innervation of mDA progenitors in the rodent PD model.
Immunohistochemical analysis of expression of HNA (magenta), TH (red), synaptophysin
(green) and DAPI (blue) in the grafts. Scale bar, 20 μm.

4. Histological analysis of grafts within the striatum of the rodent PD model

Consistent with the results of the *in vitro* differentiation process, the majority of TH+ cells co-expressed mDA neuronal markers, including FOXA2, LMX1A, and PITX3 (**Figure 10A, 10B and 10C**). A small fraction of glial fibrillary acidic protein (GFAP)+ cells was detected, making up 0.49% ±0.34% of the human cells (**Figure 11A and 11B**). Other neuronal types, such as serotonergic (5-HT+) and GABAergic (GAD65+) neurons, were scarcely detected within the graft (**Figure 11C−11F**). The graft contained only a minimal percentage of proliferative (Ki67+HNA+) cells, amounting to 1.17% ± 1.97%, and none of the non-ectodermal lineage cells (SOX17; AFP and BRACHYURY; SMAa) were identified, with no signs of abnormal overgrowth (**Figure 12A−12D**). Furthermore, non-neural contaminants, such as vascular leptomeningeal cells (COL1A1+) and choroid plexus epithelial cells (TTR+), which have been found in some mDA neuron grafts,16 were not detected within the graft (**Figure 12E**).

Taken together, these findings provide evidence that the mDA progenitors result in the production of mature and functional mDA neurons within the striatum of a PD rat model while minimizing the risk of aberrant outgrowth and the presence of unwanted cells.
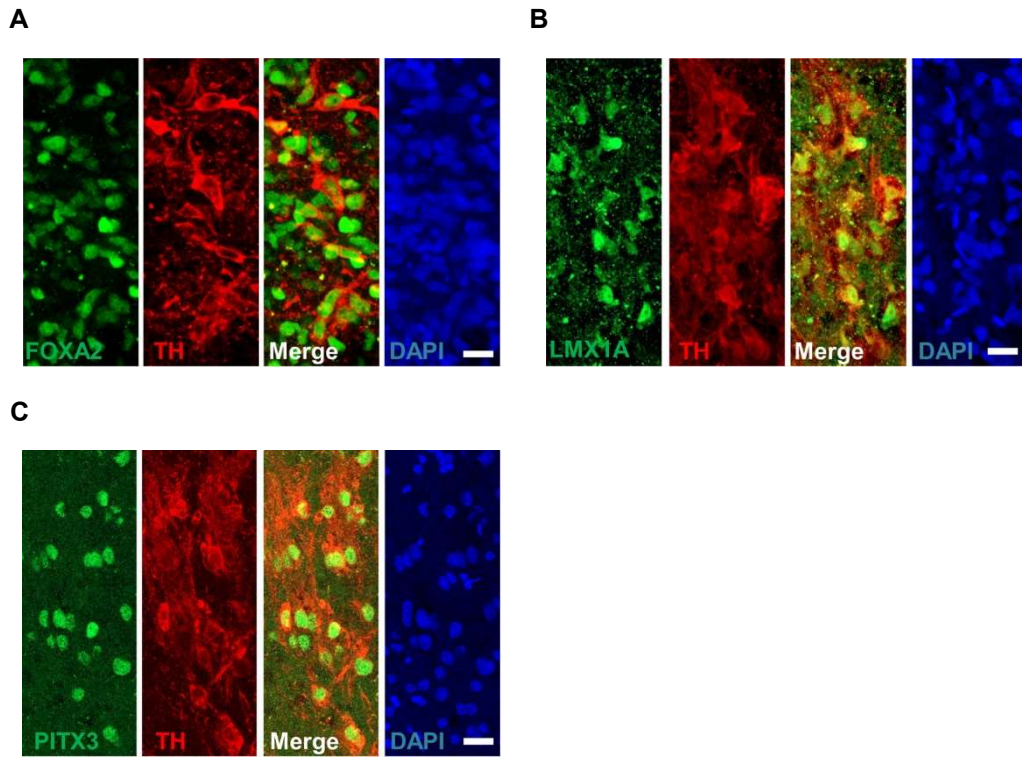
Figure 10. Histological analysis of grafts within the striatum of the rodent PD model (1). (A−C) Immunohistochemical analysis of mDA neuronal marker expression: FOXA2 (A), LMX1A (B), and PITX3 (C), with TH (red) in grafts at 16 weeks post-administration. Scale bars, 20 μm.
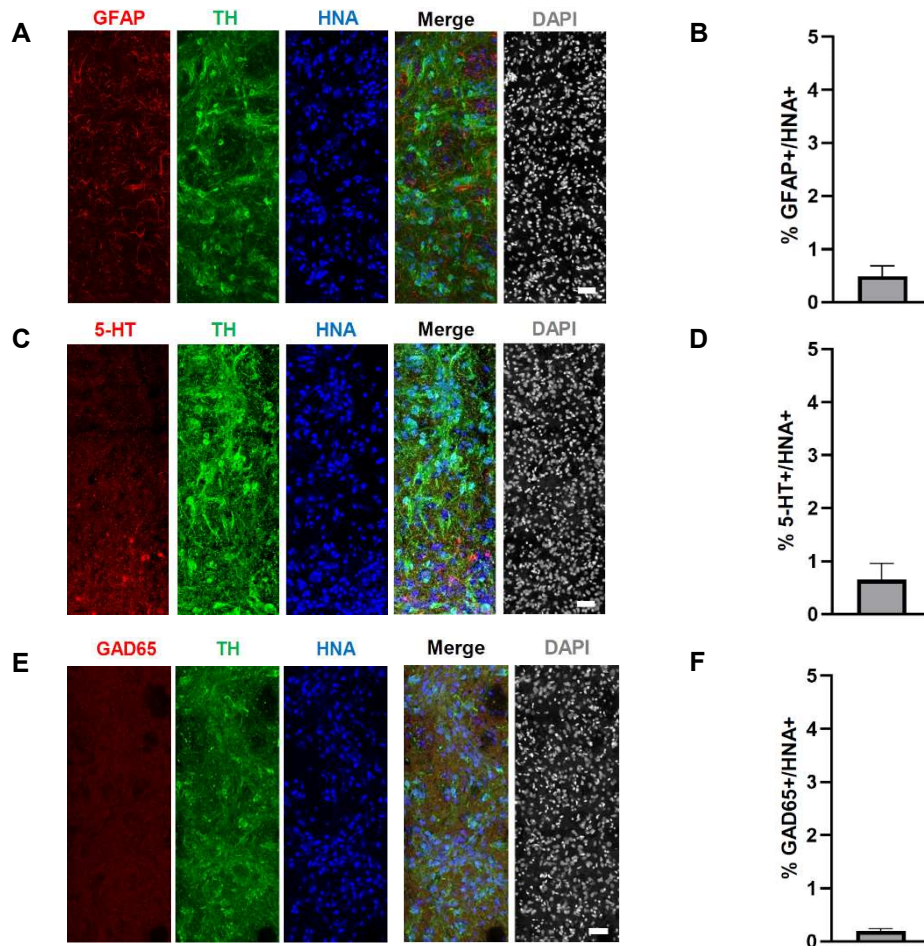
Figure 11. Histological analysis of grafts within the striatum of the rodent PD model (2). (A) Immunohistochemical analysis of expression of GFAP (red), TH (green), and HNA (blue) in the grafts. Scale bar, 50 µm. (B) Quantification of GFAP+ cells among the HNA+ cells in the grafts. Data represent the mean + SD. (C) Immunohistochemical analysis of expression of 5-HT (red), TH (green), and HNA (blue) in the grafts. Scale bar, 50 µm. (D) Quantification of 5-HT+ cells among the HNA+ cells in the grafts. Data represent the mean + SD. (E) Immunohistochemical analysis of expression of GAD65 (red), TH (green), and HNA (blue) in the grafts. Scale bar, 50 µm. (F) Quantification of GAD65 cells among the HNA+ cells in the grafts. Data represent the mean + SD.
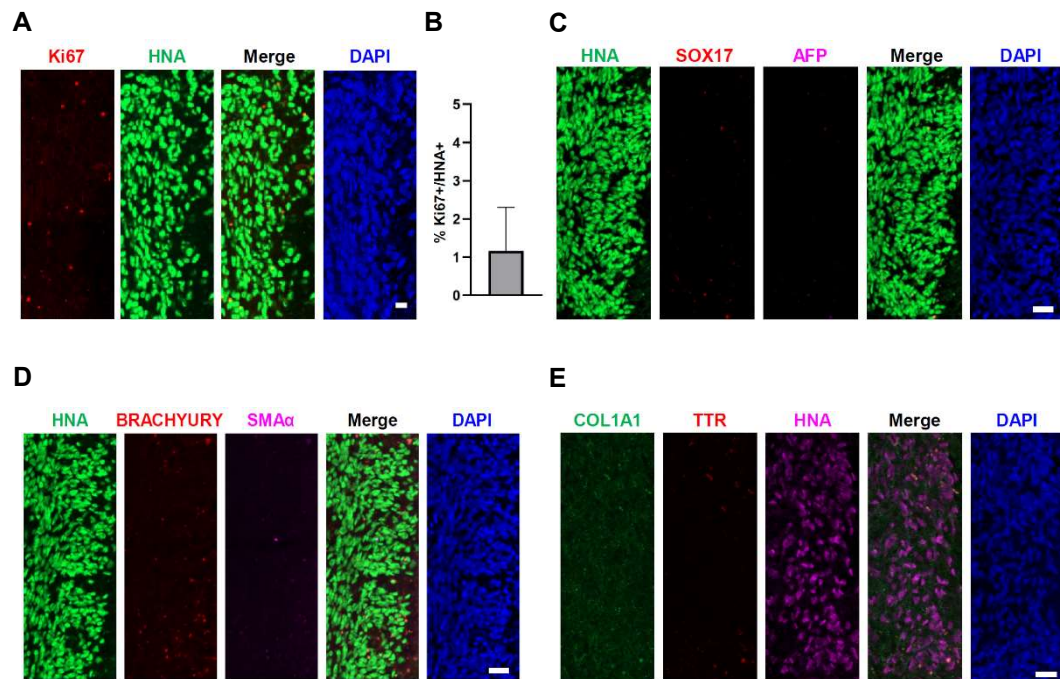
Figure 12. Histological analysis of grafts within the striatum of the rodent PD model (3). (A) Immunohistochemical analysis of expression of Ki67 (red) and HNA (green) in the grafts. Scale bar, 50 μm. (B) Quantification of Ki67+ cells among the HNA+ cells in the grafts. Data represent the mean + SD. (C) Immunohistochemical analysis of expression of HNA (green), SOX17 (red), and AFP (magenta) in the grafts. Scale bar, 50 μm. (D) Immunohistochemical analysis of expression of HNA (green), BRACHYURY (red), and SMAα (magenta) in the grafts. Scale bar, 50 μm. (E) Immunohistochemical analysis of expression of COL1A1 (green), TTR (red), and HNA (magenta) in the grafts. Scale bar, 50 μm.

5. Evaluation of the dopaminergic function of the transplanted DA progenitors

The dopamine synthesis function of the graft within the striatum was initially evaluated through PET with [^{18}F]F-DOPA. In this experiment, hemi-parkinsonian rats were tracked that received either 350,000 mDA progenitors or a vehicle injection into the right striatum. The SUVr of the right striatum was measured relative to the cerebellum, serving as a reference, using [^{18}F]F-DOPA PET scans at 4-week intervals. A significant increase in [^{18}F]F-DOPA uptake in the right striatum was observed compared with the baseline (the value measured before cell transplantation) for up to 16 weeks after cell transplantation (**Figures 13A and 13B)**. Conversely, the control group did not exhibit a significant increase in SUVr during the 16-week period. This observation reveals that the dopamine synthesis function is increased in the striatum transplanted with the mDA progenitors, suggesting that the grafts function as dopaminergic neurons.[30]

Furthermore, dopamine concentrations were assessed using HPLC equipped with PDA detection in the bilateral striatum of hemi-parkinsonian rats who had received either 350,000 mDA progenitors or a vehicle injection at 16 weeks post- transplantation. The result demonstrated that dopamine was not detected in the right striatum of any rats in the control group. However, in the cell transplantation group, the dopamine level in the right striatum was approximately 41.1% of that in the left striatum (**Figure 14)**. These findings convincingly confirm the dopamine synthesis function of the mDA progenitors, which contribute directly to behavioral enhancement by secreting dopamine into the striatum.
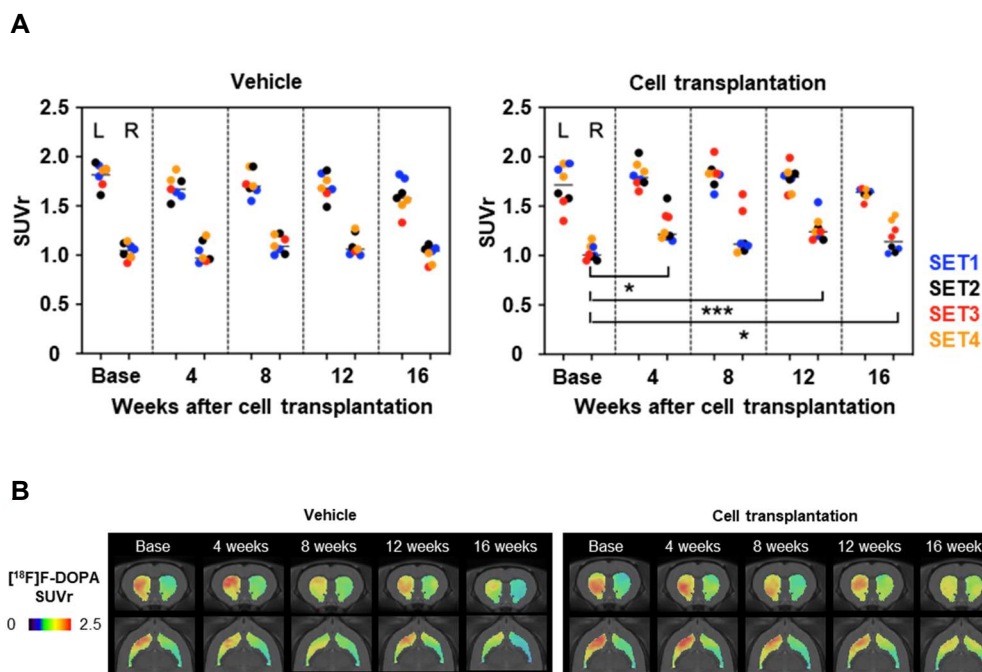
Figure 13. Evaluating the dopaminergic function of the transplanted cells with [^{18}F]F-DOPA PET scans. (A) The SUVr of the cell-transplanted group was significantly increased compared with baseline up to 16 weeks post-transplantation. In the control group, no significant change was noted up to 16 weeks. L, left striatum; R, right striatum. Data represent the mean. $^*p < 0.05$, $^{***}p < 0.001$, paired t test. (B) A representative rat of the cell-transplanted group showed increased [^{18}F]F-DOPA uptake in the right striatum until 16 weeks post-transplantation. However, a representative rat of the control group showed no significant change in [^{18}F]F-DOPA uptake in the striatum.
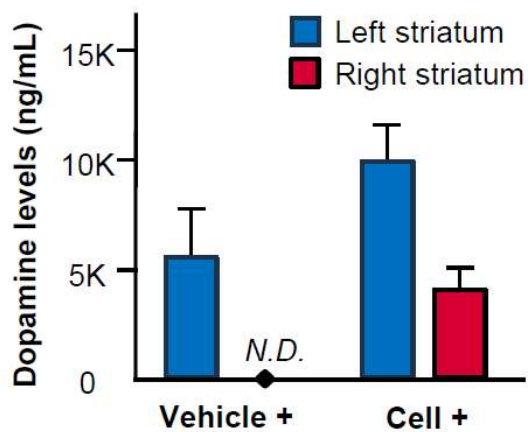
Figure 14. Evaluating the dopaminergic function of the transplanted cells with HPLC.
Dopamine levels in left and right striatum of the vehicle (n = 7) and the cell-transplanted group (n = 8) at 16 weeks post-transplantation, as measured by HPLC with PDA detection. Data represent the mean ± SD. N.D., not detected.

6. Dose response of behavioral improvement in parkinsonian rats

Next, the dose response of the mDA progenitors was explored in terms of behavioral improvement in parkinsonian rats to understand the correlation between cell dosage and functional recovery and obtain insights into the appropriate cell dose for human trials. As transplantation with 350,000 cells reversed the behavioral asymmetry of parkinsonian rats in amphetamine-induced rotation at 16 weeks (**Figure 7A)**, the mDA progenitors number was titrated down from 100,000 to 5,000 and the mDA progenitors were transplanted into the striatum of 6-OHDA lesioned rats (100,000, 25,000, 10,000, 5,000 cells; control, vehicle). In addition, the experimental period was extended up to 24 weeks to examine long-term therapeutic effects. The number of amphetamine-induced ipsilateral rotations to the lesioned site gradually decreased over time in all cell transplantation groups. Both the onset and the degree of decline correlated positively with the number of cells administered: although rats that received 100,000 cells began to show a significant decrease at 12 weeks post-transplantation, those that received 25,000 and 10,000 cells showed a significant decrease at 20 and 24 weeks, respectively (**Figure 15)**. Animals administered with 5,000 cells failed to show significant improvement by the end of the experimental period. Transplantation of 100,000 and 25,000 cells completely reversed the direction of rotation after 16 and 20 weeks, respectively. Consequently, a significant decrease in rotational asymmetry could be achieved by transplanting 10,000 or more mDA progenitors, and higher numbers of cells tended to elicit earlier and stronger recovery, indicating a clear dose-response relationship in terms of behavioral improvement.

To correlate the extent of behavioral improvement with engrafted mDA neurons in the host striatum, histological analyses were performed using TH and hNCAM immunostaining of recipients' brains (**Figure 16A and 16B**).
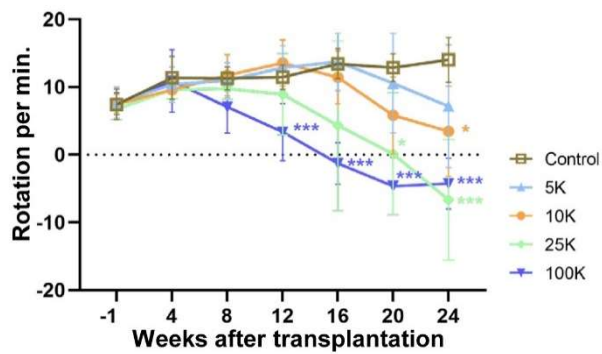
Figure 15. Dose response of behavioral improvement in parkinsonian rats. Motor behavior was measured by counting ipsilateral rotations to the lesioned site per minute at pre-transplantation (−1 week) and at 4, 8, 12, 16, 20, and 24 weeks post-transplantation. At pre-transplantation and 4 weeks post-grafting, no significant difference was noted between groups. A sequential difference in ipsilateral rotations was noted compared with the control group at 12 weeks after 100,000 cells were transplanted, 20 weeks after 25,000 cells were transplanted, and 24 weeks after 10,000 cells were transplanted. Data represent the mean ± SD. $^{*}p < 0.05$, $^{***}p < 0.001$, one-way ANOVA with Bonferroni post hoc test. 100K, 100,000 cells; 25K, 25,000 cells; 10K, 10,000 cells; 5K, 5,000 cells; control, vehicle.
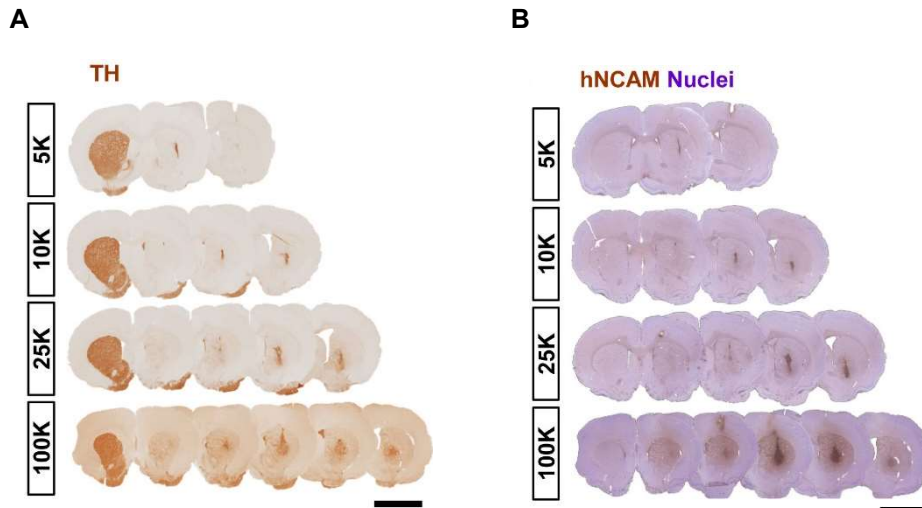
Figure 16. DAB-staining in the grafts within the host striatum of each graft group. (A and B) Representative images of TH/DAB (A) and hNCAM/DAB and hematoxylin-stained (B) coronal sections of each graft group (5,000, 10,000, 25,000, and 100,000 cells). Scale bars, 5 mm.

7. The restoration of behavior is likely due to the functional innervation of the dorsal striatum by transplanted neurons

The DA fiber volume in the NAc and the DS of the cell-injected hemisphere was first quantified,[31] two regions associated with the amphetamine-induced rotation test.[32] These regions were manually identified in each brain section using the rat brain atlas (**Figure 17A**).[26] The DA fiber volume in the NAc correlated weakly with cell dosages, whereas that in the DS correlated strongly with cell dosage based on a linear regression test (DS, $r^2 = 0.727$, $p < 0.001$; NAc, $r^2 = 0.399$, $p < 0.001$) (**Figure 17B and 17C**). The correlation between the rotations per minute at 24 weeks post-transplantation and the DA fiber volume in the DS or NAc was statistically analyzed. A logarithmic regression model (DS, $r^2 = 0.585$, $p < 0.001$; NAc, $r^2 = 0.251$, $p < 0.01$) fit better than a linear regression model (DS, $r^2 = 0.284$, $p < 0.01$; NAc, $r^2 = 0.178$, $p < 0.05$) (**Figure 18A and 18B**). Based on the logarithmic regression model, the DA fiber volume in the DS correlated more strongly with the behavior test results than did that in the NAc. These results imply that the innervation of neurons in the DS by the transplanted mDA neurons had a greater impact on the observed behavioral improvement than did their unintended synaptic targets in the NAc.[33] Therefore, the beneficial effects observed were likely due to the functional innervation of the DS by transplanted neurons in host brain circuits.

A

☐ Dorsal striatum (DS)
☐ Nucleus accumbens (NAc)

B

C
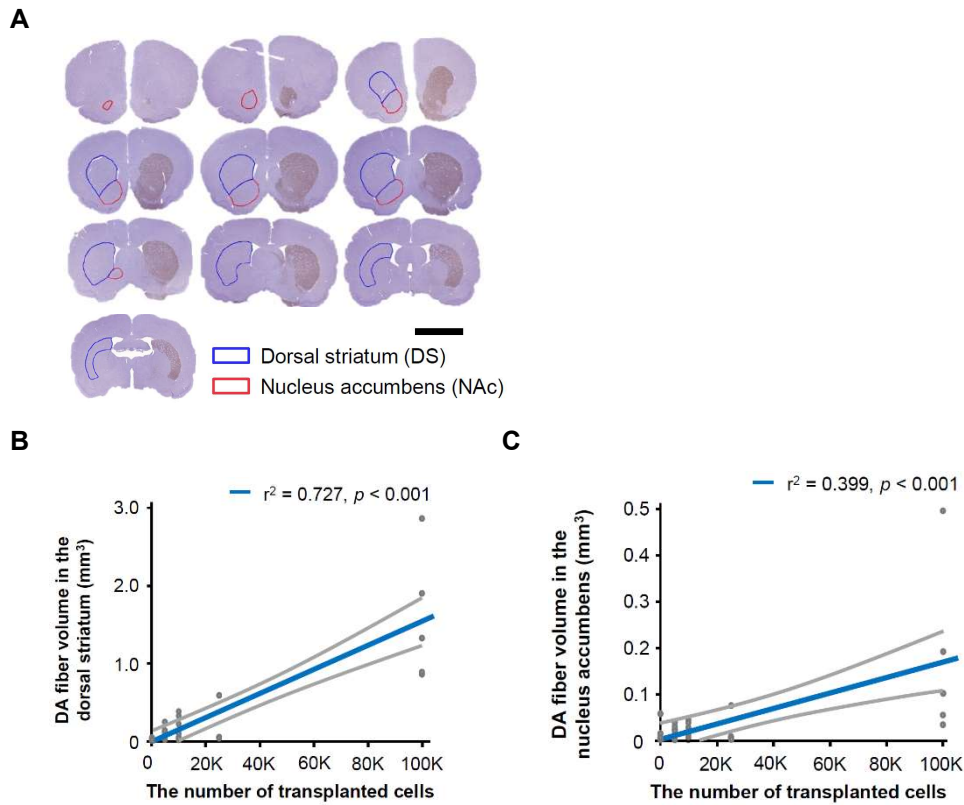
Figure 17. Correlation between DA fiber volume and the number of transplanted cells in parkinsonian rats. (A) The NAc (red line) and the DS (blue line) of the rat brain at each brain section are defined by the rat brain atlas. Scale bar, 5 mm. (B–C) Calculated dopaminergic fiber volume in the DS (B) and the NAc (C) of the grafted site plotted against the number of transplanted cells. Linear regression with 95% confidence intervals for the number of transplanted cells and dopaminergic fiber volume in the DS or NAc. K, thousand

A

B
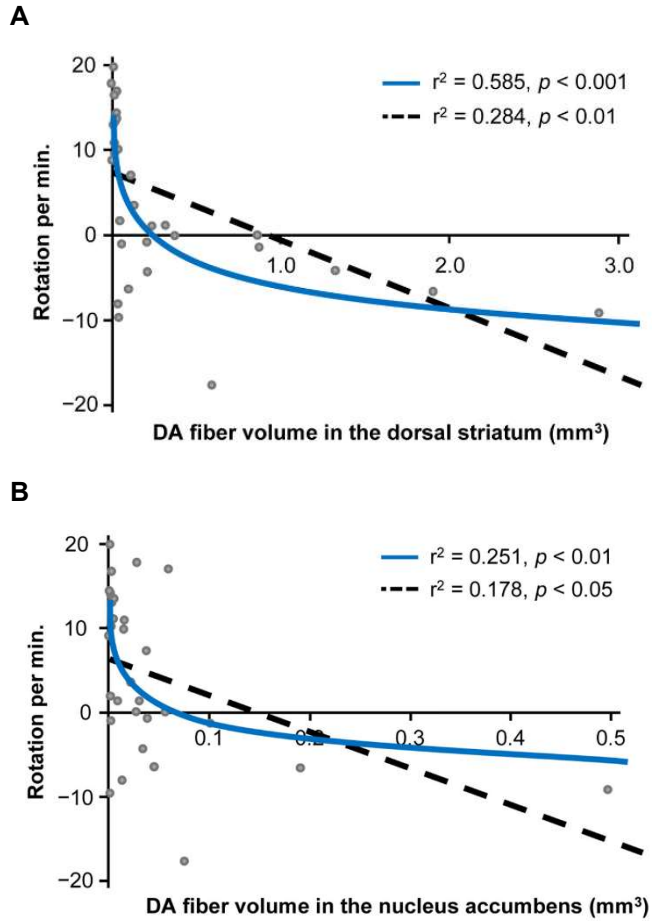
Figure 18. Correlation between DA fiber volume and behavioral improvement in parkinsonian rats. (A and B) Ipsilateral rotations to the lesioned site per minute plotted against calculated DA fiber volume in the DS (A) and NAc (B) of the grafted site. Logarithmic and linear regression for DS or NAc and ipsilateral rotations.

8. Quantification of the number of surviving cells and mDA neurons

To investigate the relationship between the cell dosage and the graft-induced functional improvement further, the total number of surviving cells (HNA+ cells) and mDA neurons (HNA+TH+ cells) were quantified after immunostaining of striatal regions (**Figure 19A−19C**). Stereological quantification revealed that the average number of surviving human (HNA+) cells in the graft varied across groups: 2,717.71 ± 1,074.95, 7,804.57 ± 4,138.67, 8,294.00 ± 1,189.22, and a remarkable 126,646.40 ± 57,655.85 HNA+ cells in the 5,000, 10,000, 25,000, and 100,000 groups, respectively (**Figure 19B**). These grafts also contained an average of 758.86 ± 286.00 (5,000 group), 1,477.71 ± 529.79 (10,000 group), 2,820.00 ± 1,378.86 (25,000 group), and 17,598.40 ± 5,451.54 (100,000 group) TH+ DA neurons (**Figure 19C**).
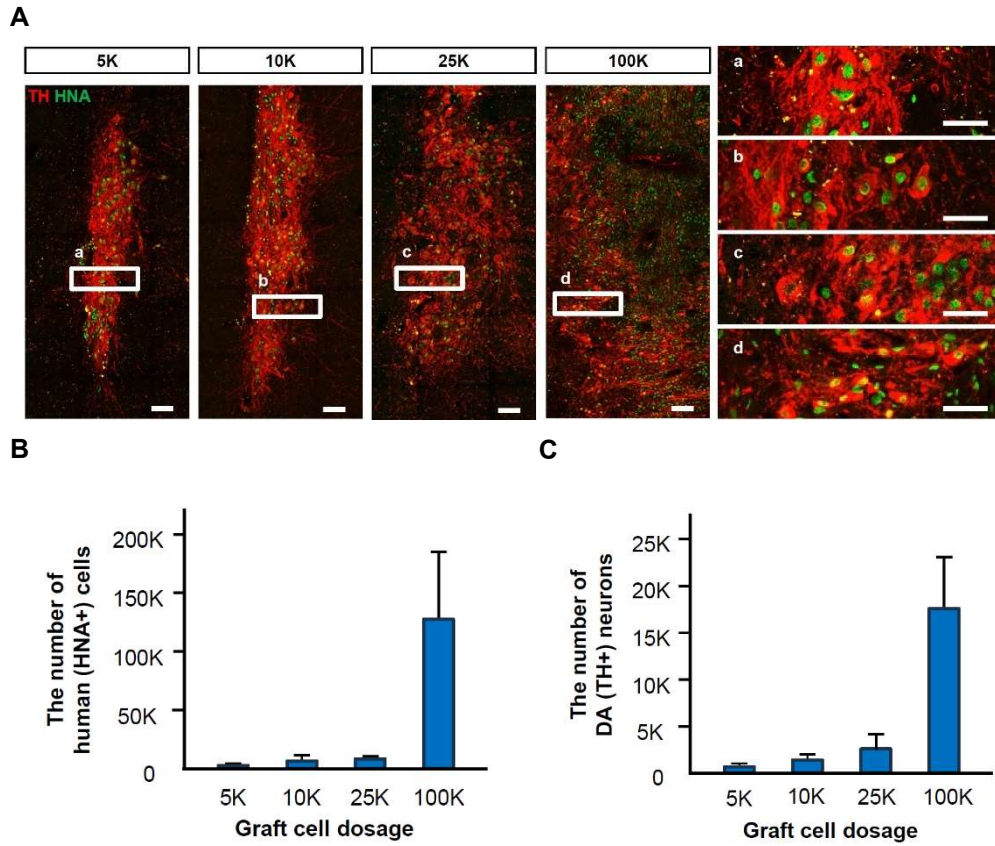
Figure 19. Dose-escalation study of mDA progenitors in the rodent PD models. (A) Representative immunohistochemical images of TH (red) and HNA (green) in graft group (5,000, 10,000, 25,000, and 100,000 cells) at 24 weeks after administration. Scale bars in the low-magnification images, 100 μm; Scale bars in the high-magnification images, 50 μm. (B–C) The number of surviving human (HNA+) cells (B) and DA (TH+) neurons (C) in each graft group (5,000, 10,000, 25,000, and 100,000 cells). Data present the mean + SE.

9. Dose-escalation study of mDA progenitors in the rodent PD models

As expected, the total numbers of surviving cells increased linearly with cell dose ($r^2 = 0.449$, $p < 0.001$) (**Figure 20A**), with the number of mDA neurons showing a stronger correlation with cell dose ($r^2 = 0.614$, $p < 0.001$) (**Figure 20B**). The number of surviving cells correlated with the degree of ipsilateral rotations measured at 24 weeks post-transplantation. However, this relationship was not linear. Instead, logarithmic regression analysis was applied (HNA+ cells, $r^2 = 0.404$, $p < 0.005$) (**Figure 21A**). The numbers of mDA neurons exhibited a stronger correlation with the motor behavior test results than did the total number of surviving cells (HNA+TH+ cells, $r^2 = 0.589$, $p < 0.001$) (**Figure 21B**). Notably, when the groups were divided into low dose (5,000 and 10,000 cells) and high dose (25,000 and 100,000 cells), a moderate logarithmic relationship between the number of mDA neurons and ipsilateral rotations was observed in the low-dose group ($r^2 = 0.641$, $p < 0.005$) (**Figure 22A**). In contrast, no significant correlation was found between these two factors in the high-dose group ($r^2 = 0.020$, $p = 0.716$) (**Figure 22B**). When the total number of surviving DA neurons (HNA+TH+ cells) was estimated based on the number of transplanted cells, no difference among different dosage groups was found, and the mean value was 14.9% ± 12.8% (**Figure 23**). These results indicate that elevating the cell dose led to a concomitant increase in the number of surviving DA neurons within the graft. However, this increase did not cause a proportional enhancement in the motor function of the PD model rats, implying that once the number of DA neurons in the graft reached a specific threshold, not all additional cells could further improve the behavioral outcomes

in the amphetamine-induced rotation test. This was similar to the so-called ''ceiling effect'' described previously.[34]
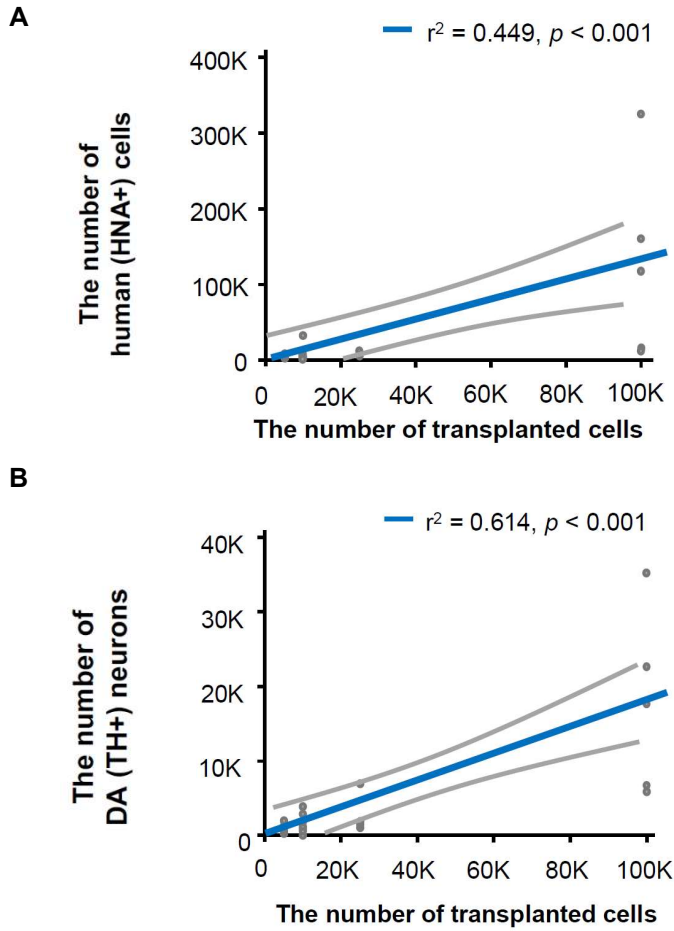
Figure 20. Correlation between the number of transplanted cells and the number of human cells or DA neurons in parkinsonian rats. (A–B) The number of human (HNA+) cells (A) and DA (TH+) neurons (B) plotted against the number of transplanted cells. Linear regression with a 95% confidence interval for the number of transplanted cells and the number of human cells or DA neurons.

A

B
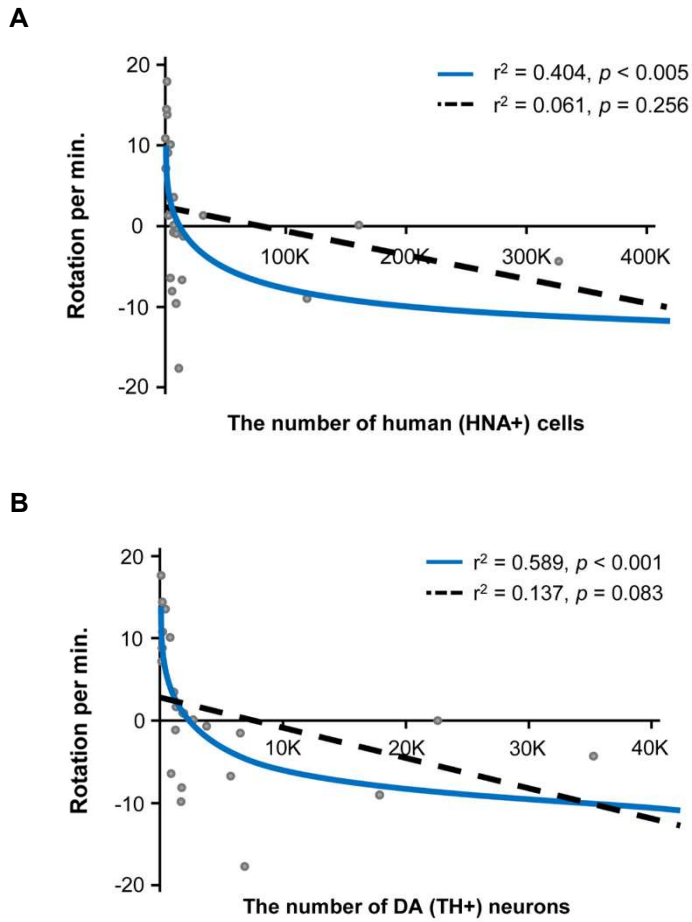
Figure 21. Correlation between the number of human cells or DA neurons and behavioral improvement in parkinsonian rats. (A and B) Ipsilateral rotations to the lesioned site per minute plotted against grafted cell (HNA+) number (A) and grafted DA neuron (HNA+TH+) number (B). Logarithmic and linear regression for grafted cell or DA neuron number and ipsilateral rotations are shown. K, thousand.

A

B
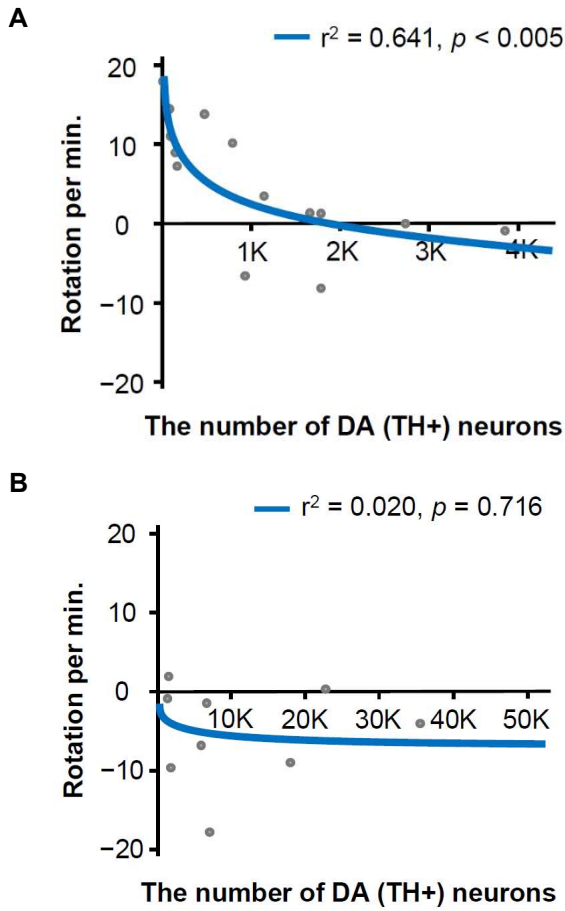
Figure 22. Correlation between the number of DA neurons of low or high dose group and behavioral improvement in parkinsonian rats. (A and B) Ipsilateral rotations to the lesioned site per minute plotted against the number of DA (TH+) neurons of low-dose groups (5,000 and 10,000 cells) (A) and high-dose groups (25,000 and 100,000 cells) (B). Logarithmic regression for the number of DA neurons of the low- or high-dose group and ipsilateral rotations is shown.
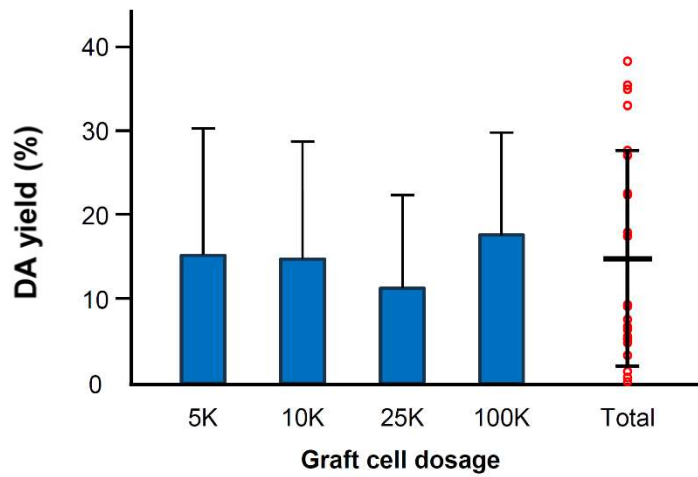
Figure 23. DA yield of each group. Percentage of surviving DA (HNA+TH+) neurons to the number of transplanted cells (DA yield). Data represent the mean ± SD. In this figure, the numbers of subjects in each group are as follows: control, 9; 5,000 cells, 7; 10,000 cells, 7; 25,000 cells, 4; 100,000 cells, 5.

IV. DISCUSSION

In this study, I presented the differentiation protocol to produce high purity mDA progenitors with the results of preclinical *in vivo* assessments for efficacy, and explored the range of cell doses showing therapeutic effects in a PD rat model.

A robust differentiation protocol for mDA progenitors was developed. The fine modulation of signaling pathways for neural induction and regional (ventral mesencephalic) patterning was achieved by exclusively utilizing small molecules and carefully modifying the timing and concentration of their use. When transplanted into 6-OHDA lesioned SD rat models, the mDA progenitors integrated and differentiated into functional TH+ DA neurons in the host brains, resulting in complete normalization of amphetamine-induced motor asymmetry with increased [^{18}F]F-DOPA uptake on PET and HPLC-determined DA concentration at 16 weeks post-transplantation. Histochemical analysis showed that only 1.17% of the cells in the population were Ki67+, and no evidence of aberrant proliferation was found in the grafts. Collectively, these results indicate that the mDA progenitors are highly effective in restoring motor deficits in parkinsonian rats, with an extremely low risk of abnormal overgrowth and graft-induced dyskinesia.

It is necessary to determine the range of effective cell doses before conducting clinical trials, as exposure to subtherapeutic or supratherapeutic doses must be avoided to ensure the efficacy and safety of human subjects. Consequently, the dose response of the mDA progenitors in rat PD models was investigated. A clear dose response in the

behavioral recovery profile was observed in the range of 5,000–100,000 cells. A significant reduction in the number of amphetamine-induced rotations first appeared in animals that received 100,000 mDA progenitors, followed by those that received fewer cells. By the end of the test period, all transplantation groups, except for the group that received 5,000 cells, which also displayed a distinct trend of reduced rotation numbers, showed significant behavioral recovery. Based on the results, it can be concluded that in the rat PD model based on the amphetamine-induced rotation test, the minimum effective therapeutic cell dose for the mDA progenitors lies within the range of 5,000–10,000 cells per hemisphere.

Given the volume ratio of rat and human striata (1:187),[35-43] the low-dose range per hemisphere determined for the rat model corresponds to a range of 1.87–3.74 million cells for human whole brain. The estimated range of grafted DA neurons per putamen (hemisphere), based on the mean survival rate of DA neurons (approximately 15%, **Figure 11G**) and the range of graft cell dose (1.87–3.74 million mDA progenitors for human whole brain), is approximately 0.14–0.28 million cells. Previous postmortem analyses of PD patients' brains that had received fetal nigral transplantation indicated that clinical improvement was observed in patients who received approximately 0.1 million DA neurons per putamen.[7, 44-46] Considering the challenging brain environment in PD patients, a dose of surviving DA neurons of more than 0.10 million per putamen is recommended. Therefore, a range of 1.87–3.74 million mDA progenitors (0.14–0.28 million DA neurons/putamen) are within the recommendation for human transplantation. Thus, this study offers insights into the minimum effective dose range for human trials: a dose of 3.15

million cells is considered low for human clinical trials.

V. CONCLUSION

This study developed a robust differentiation protocol for ventral mDA progenitors, demonstrating successful differentiation into functional mDA neurons in PD rat models. Immunohistochemical analysis showed low proliferation and no abnormal growth, ensuring safety. Minimal cell dose range for therapeutic effect was determined to be 5,000–10,000 cells per hemisphere in rats, translating to 1.87–3.74 million cells for humans.

References

1. de Lau LM, Breteler MM. Epidemiology of Parkinson's disease. Lancet Neurol. 2006 Jun;5(6):525-35.

2. Armstrong MJ, Okun MS. Diagnosis and Treatment of Parkinson Disease: A Review. Jama. 2020 Feb 11;323(6):548-60.

3. Madrazo I, León V, Torres C, Aguilera MC, Varela G, Alvarez F, et al. Transplantation of fetal substantia nigra and adrenal medulla to the caudate nucleus in two patients with Parkinson's disease. N Engl J Med. 1988 Jan 7;318(1):51.

4. Lindvall O, Rehncrona S, Gustavii B, Brundin P, Astedt B, Widner H, et al. Fetal dopamine-rich mesencephalic grafts in Parkinson's disease. Lancet. 1988 Dec 24-31;2(8626-8627):1483-4.

5. Yasuhara T, Kameda M, Sasaki T, Tajiri N, Date I. Cell Therapy for Parkinson's Disease. Cell Transplant. 2017 Sep;26(9):1551-9.

6. Olanow CW, Goetz CG, Kordower JH, Stoessl AJ, Sossi V, Brin MF, et al. A double-blind controlled trial of bilateral fetal nigral transplantation in Parkinson's disease. Ann Neurol. 2003 Sep;54(3):403-14.

7. Mendez I, Sanchez-Pernaute R, Cooper O, Viñuela A, Ferrari D, Björklund L, et al. Cell type analysis of functional fetal dopamine cell suspension transplants in the striatum and substantia nigra of patients with Parkinson's disease. Brain. 2005 Jul;128(Pt 7):1498-510.

8. Bjorklund A, Kordower JH. Cell therapy for Parkinson's disease: what next? Mov Disord. 2013 Jan;28(1):110-5.

9. Roy NS, Cleren C, Singh SK, Yang L, Beal MF, Goldman SA. Functional engraftment of human ES cell-derived dopaminergic neurons enriched by coculture with telomerase-immortalized midbrain astrocytes. Nat Med. 2006 Nov;12(11):1259-68.

10. Cho MS, Hwang DY, Kim DW. Efficient derivation of functional dopaminergic neurons from human embryonic stem cells on a large scale. Nat Protoc. 2008;3(12):1888-94.

11. Cho MS, Lee YE, Kim JY, Chung S, Cho YH, Kim DS, et al. Highly efficient and large-scale generation of functional dopamine neurons from human embryonic stem cells. Proc Natl Acad Sci U S A. 2008 Mar 4;105(9):3392-7.

12. Skidmore S, Barker RA. Challenges in the clinical advancement of cell therapies for Parkinson's disease. Nat Biomed Eng. 2023 Jan 12.

13. Sonntag KC, Song B, Lee N, Jung JH, Cha Y, Leblanc P, et al. Pluripotent stem cell-based therapy for Parkinson's disease: Current status and future prospects. Prog Neurobiol. 2018 Sep;168:1-20.

14. Kim TW, Koo SY, Studer L. Pluripotent Stem Cell Therapies for Parkinson Disease: Present Challenges and Future Opportunities. Front Cell Dev Biol. 2020;8:729.

15. Chambers SM, Qi Y, Mica Y, Lee G, Zhang XJ, Niu L, et al. Combined small-molecule inhibition accelerates developmental timing and converts human pluripotent stem cells into nociceptors. Nat Biotechnol. 2012 Jul 1;30(7):715-20.

16. Li H, Jiang H, Li H, Li L, Yan Z, Feng J. Generation of human A9 dopaminergic pacemakers from induced pluripotent stem cells. Mol Psychiatry. 2022 Nov;27(11):4407-18.

17. Yoo JE, Lee DR, Park S, Shin HR, Lee KG, Kim DS, et al. Trophoblast glycoprotein is a marker for efficient sorting of ventral mesencephalic dopaminergic precursors derived from human pluripotent stem cells. NPJ Parkinsons Dis. 2021 Jul 19;7(1):61.

18. Kikuchi T, Morizane A, Doi D, Magotani H, Onoe H, Hayashi T, et al. Human iPS cell-derived

dopaminergic neurons function in a primate Parkinson's disease model. Nature. 2017 Aug 30;548(7669):592-6.

19. Xiong M, Tao Y, Gao Q, Feng B, Yan W, Zhou Y, et al. Human Stem Cell-Derived Neurons Repair Circuits and Restore Neural Function. Cell Stem Cell. 2021 Jan 7;28(1):112-26.e6.

20. Schweitzer JS, Song B, Herrington TM, Park TY, Lee N, Ko S, et al. Personalized iPSC-Derived Dopamine Progenitor Cells for Parkinson's Disease. N Engl J Med. 2020 May 14;382(20):1926-32.

21. Doi D, Magotani H, Kikuchi T, Ikeda M, Hiramatsu S, Yoshida K, et al. Pre-clinical study of induced pluripotent stem cell-derived dopaminergic progenitor cells for Parkinson's disease. Nat Commun. 2020 Jul 6;11(1):3369.

22. Piao J, Zabierowski S, Dubose BN, Hill EJ, Navare M, Claros N, et al. Preclinical Efficacy and Safety of a Human Embryonic Stem Cell-Derived Midbrain Dopamine Progenitor Product, MSK-DA01. Cell Stem Cell. 2021 Feb 4;28(2):217-29.e7.

23. Kirkeby A, Nelander J, Hoban DB, Rogelius N, Bjartmarz H, Storm P, et al. Preclinical quality, safety, and efficacy of a human embryonic stem cell-derived product for the treatment of Parkinson's disease, STEM-PD. Cell Stem Cell. 2023 Oct 5;30(10):1299-314.e9.

24. Abercrombie M. Estimation of nuclear population from microtome sections. Anat Rec. 1946 Feb;94:239-47.

25. von Bartheld C. Counting particles in tissue sections: choices of methods and importance of calibration to minimize biases. Histol Histopathol. 2002 Apr;17(2):639-48.

26. George P, Charles W, Evan C, Alexandra B, Johnson GA. MRI/DTI Atlas of the Rat Brain. London: Academic Press; 2015.

27. Dunn WD, Jr., Gearing M, Park Y, Zhang L, Hanfelt J, Glass JD, et al. Applicability of digital analysis and imaging technology in neuropathology assessment. Neuropathology. 2016 Jun;36(3):270-82.

28. Garcia Y, Breen A, Burugapalli K, Dockery P, Pandit A. Stereological methods to assess tissue response for tissue-engineered scaffolds. Biomaterials. 2007 Jan;28(2):175-86.

29. Gu MJ, Jeon JH, Oh MS, Hong SP. Measuring levels of biogenic amines and their metabolites in rat brain tissue using high-performance liquid chromatography with photodiode array detection. Arch Pharm Res. 2016 Jan;39(1):59-65.

30. Kyono K, Takashima T, Katayama Y, Kawasaki T, Zochi R, Gouda M, et al. Use of [18F]FDOPA-PET for in vivo evaluation of dopaminergic dysfunction in unilaterally 6-OHDA-lesioned rats. EJNMMI Res. 2011 Nov 10;1(1):25.

31. Matsuda W, Furuta T, Nakamura KC, Hioki H, Fujiyama F, Arai R, et al. Single nigrostriatal dopaminergic neurons form widely spread and highly dense axonal arborizations in the neostriatum. J Neurosci. 2009 Jan 14;29(2):444-53.

32. Björklund A, Dunnett SB. The Amphetamine Induced Rotation Test: A Re-Assessment of Its Use as a Tool to Monitor Motor Impairment and Functional Recovery in Rodent Models of Parkinson's Disease. J Parkinsons Dis. 2019;9(1):17-29.

33. Grealish S, Jönsson ME, Li M, Kirik D, Björklund A, Thompson LH. The A9 dopamine neuron component in grafts of ventral mesencephalon is an important determinant for recovery of motor function in a rat model of Parkinson's disease. Brain. 2010 Feb;133(Pt 2):482-95.

34. Hiller BM, Marmion DJ, Thompson CA, Elliott NA, Federoff H, Brundin P, et al. Optimizing maturity and dose of iPSC-derived dopamine progenitor cell therapy for Parkinson's disease. NPJ Regen Med. 2022 Apr 21;7(1):24.

35. Andersson C, Hamer RM, Lawler CP, Mailman RB, Lieberman JA. Striatal volume changes in the rat following long-term administration of typical and atypical antipsychotic drugs. Neuropsychopharmacology. 2002 Aug;27(2):143-51.

36. Pitcher TL, Melzer TR, Macaskill MR, Graham CF, Livingston L, Keenan RJ, et al. Reduced striatal volumes in Parkinson's disease: a magnetic resonance imaging study. Transl Neurodegener. 2012 Aug 21;1(1):17.

37. Abedelahi A, Hasanzadeh H, Hadizadeh H, Joghataie MT. Morphometric and volumetric study of caudate and putamen nuclei in normal individuals by MRI: Effect of normal aging, gender and hemispheric differences. Pol J Radiol. 2013 Jul;78(3):7-14.

38. Wong JE, Cao J, Dorris DM, Meitzen J. Genetic sex and the volumes of the caudate-putamen, nucleus accumbens core and shell: original data and a review. Brain Struct Funct. 2016 Nov;221(8):4257-67.

39. Hamezah HS, Durani LW, Ibrahim NF, Yanagisawa D, Kato T, Shiino A, et al. Volumetric changes in the aging rat brain and its impact on cognitive and locomotor functions. Exp Gerontol. 2017 Dec 1;99:69-79.

40. Welniak-Kaminska M, Fiedorowicz M, Orzel J, Bogorodzki P, Modlinska K, Stryjek R, et al. Volumes of brain structures in captive wild-type and laboratory rats: 7T magnetic resonance in vivo automatic atlas-based study. PLoS One. 2019;14(4):e0215348.

41. Thanos PK, Kim R, Delis F, Ananth M, Chachati G, Rocco MJ, et al. Chronic Methamphetamine Effects on Brain Structure and Function in Rats. PLoS One. 2016;11(6):e0155457.

42. Mengler L, Khmelinskii A, Diedenhofen M, Po C, Staring M, Lelieveldt BP, et al. Brain maturation of the adolescent rat cortex and striatum: changes in volume and myelination. Neuroimage. 2014 Jan 1;84:35-44.

43. Nguyen HP, Kobbe P, Rahne H, Wörpel T, Jäger B, Stephan M, et al. Behavioral abnormalities precede neuropathological markers in rats transgenic for Huntington's disease. Hum Mol Genet. 2006 Nov 1;15(21):3177-94.

44. Hauser RA, Freeman TB, Snow BJ, Nauert M, Gauger L, Kordower JH, et al. Long-term evaluation of bilateral fetal nigral transplantation in Parkinson disease. Arch Neurol. 1999 Feb;56(2):179-87.

45. Kordower JH, Rosenstein JM, Collier TJ, Burke MA, Chen EY, Li JM, et al. Functional fetal nigral grafts in a patient with Parkinson's disease: chemoanatomic, ultrastructural, and metabolic studies. J Comp Neurol. 1996 Jun 24;370(2):203-30.

46. Li JY, Englund E, Holton JL, Soulet D, Hagell P, Lees AJ, et al. Lewy bodies in grafted neurons in subjects with Parkinson's disease suggest host-to-graft disease propagation. Nat Med. 2008 May;14(5):501-3.

PUBLICATION LIST

Park S, Park CW, Eom JH, Jo MY, Hur HJ, Choi SK, et al. Preclinical and dose-ranging assessment of hESC-derived dopaminergic progenitors for a clinical trial on Parkinson's disease. Cell Stem Cell. 2024 Jan 4;31(1):25-38.e8.

APPENDIX

본 학위논문은 이미 발표 및 출판된 논문을 재구성하여 작성되었으며, 텍스트 및 데이터 재사용에 대한 출판사(Elsevier)의 동의를 얻었음을 명시함.

This dissertation was reconstituted from a previously published article, with official agreement from the publisher (Elsevier) for re-use of the full text and data.

Park S, Park CW, Eom JH, Jo MY, Hur HJ, Choi SK, et al. Preclinical and dose-ranging assessment of hESC-derived dopaminergic progenitors for a clinical trial on Parkinson's disease. Cell Stem Cell. 2024 Jan 4;31(1):25-38.e8.

Abstract in Korean

파킨슨병 치료를 위한 인간 전분화능 줄기세포 유래 중뇌 도파민 신경세포 분화 및 용량 범위 평가

인간 전분화능 줄기세포로부터 유래한 중뇌 도파민 전구세포 이식은 파킨슨병 치료에 있어 유망한 전략으로 알려져 있다. 이러한 세포 치료의 임상 적용을 위해서는 인간 전분화능 줄기세포로부터 높은 안전성과 효능을 가진 도파민 전구세포를 생산하는 분화 방법을 개발하는 것이 중요하다. 이번 연구에서는 dual-SMAD 억제와 smoothened agonist (SAG) 및 CHIR99021을 포함한 네 가지 저분자 화합물을 사용하여 인간 배아줄기세포로부터 고순도 중뇌 도파민 전구세포를 생산하는 분화 프로토콜을 개발했다. 전임상 평가 결과, 편측 파킨슨병 쥐 모델에 이식된 도파민 전구세포가 기능적인 도파민 신경세포로 분화하여 뇌에 생착하는 것을 확인하였다. 이식된 도파민 신경세포는 이식 후 16주 시점에서 파킨슨병 쥐의 운동 기능을 정상화시키고, $[^{18}F]$F-DOPA 섭취 및 도파민 양을 증가시키는 것을 확인할 수 있었다. 면역조직화학 분석에서는 이식된 도파민 전구세포의 증식률이 낮고 비정상적인 증식이 없음을 관찰하여 안전성을 확인했다. 또한 임상 시험을 진행하기 전에 치료 효과를 가진 최저 세포 용량의 범위를 결정하는 것이 필수적이다. 편측 파킨슨병 쥐 모델에 다양한 용량의 중뇌 도파민 전구세포를 이식하였을 때 용량에 따른 행동 개선이 나타났고, 효과를 보이는 최소한의 세포 용량은 5,000개에서 10,000개 사이로 관찰되었다. 이러한 결과는 인간 임상 시험에 사용될 세포의 최소 용량인 315만개를 결정하는 데 중요한 기준을 제공했다.

_____

핵심되는 말: 파킨슨병; 인간 전분화능 줄기세포; 도파민 세포 분화; 세포 이식; 용량 증량 연구